Condensed Complexes and the Calorimetry of Cholesterol-Phospholipid Bilayers

Thomas G. Anderson and Harden M. McConnell
Department of Chemistry, Stanford University, Stanford, California 94305 USA

ABSTRACT   A recent thermodynamic model describes a reversible reaction between cholesterol (C) and phospholipid (P) to form a *condensed complex* $C_{nq}P_{np}$. Here q and p are relatively prime integers used to define the stoichiometric composition, and n is a measure of cooperativity. The present study applies this model to the scanning calorimetry of binary mixtures of cholesterol and saturated phosphatidylcholines, especially work by McElhaney and collaborators. These mixtures generally show two heat capacity peaks, a sharp peak and a broad peak. The sharp heat absorption is largely due to the chain melting transition of pure phospholipid. In the present work the broad heat absorption is attributed to the thermal dissociation of complexes. The best fits of the model to the data require the complex formation to be highly cooperative, with cooperativity $n = 12$. Detailed comparisons are made between model calculations and calorimetric data. A number of unusual features of the data arise naturally in the model. The principal discrepancy between the calculations and experimental results is a spurious calculated heat absorption peak. This discrepancy is related to the reported relative magnitudes of the integrated broad and sharp heat absorption curves.

INTRODUCTION

There are numerous studies of binary mixtures of cholesterol and phosphatidylcholines using differential scanning calorimetry (DSC). Much of this work is summarized by Feingold (1993). Binary mixtures of cholesterol and dipalmitoylphosphatidylcholine (DPPC) have been studied most often. The DSC of this and other cholesterol-phospholipid mixtures has supported the view that these mixtures are far from ideal, a view that originated from early observations of the "condensing effect" of cholesterol in mixtures with lipids in monolayers at the air-water interface. In monolayers this condensing effect is manifested by deviations from additivity of molecular areas (Leathes, 1925). In DSC the deviations from ideality appear most directly as a deviation from ideal melting point depression, for example in cholesterol-DPPC mixtures (Hinz and Sturtevant, 1972). Aqueous dispersions of pure DPPC bilayers show a sharp solid-to-liquid chain melting transition at 41°C. In the presence of increasing concentrations of cholesterol, the temperature of this transition decreases less rapidly than would be expected if cholesterol formed an ideal mixture with DPPC in the liquid phase and did not dissolve in the DPPC solid phase. The sharp heat absorption peak associated with the chain melting decreases in amplitude and disappears at ~20–25% cholesterol. In addition, a broad heat absorption is found at higher temperatures, whose temperature maximum and integrated enthalpy depend on the bilayer composition (Hinz and Sturtevant, 1972; Feingold, 1993). These earlier studies have been significantly extended by Mc-Mullen et al. (1993). They investigated binary mixtures of

cholesterol and a series of phosphatidylcholines with various saturated fatty acid chain lengths. In their work the DSC curves for dimyristoylphosphatidylcholine (DMPC, 14 carbons), DPPC (16 carbons), distearoylphosphatidylcholine (DSPC, 18 carbons), and diarachidoylphosphatidylcholine (DAPC, 20 carbons) were analyzed quantitatively with respect to the cholesterol concentration dependence of the sharp and broad heat absorptions.

A thermodynamic phase diagram has been proposed to account for the DSC and other properties of cholesterol-phosphatidylcholine mixtures (Thewalt and Bloom, 1992; Ipsen et al., 1987). Phase diagrams have been based on experimental work and theoretical modeling (Nielsen et al., 1999; Vist and Davis, 1989). Early proposals for the formation of complexes between cholesterol and phospholipids have been extended to include lattice-like models involving ordered arrays of cholesterol and phospholipid molecules (Finean, 1953; Mabrey et al., 1978; Presti et al., 1982; Sugar et al., 1994; Wang et al., 1998; Somerharju et al., 1999). For x-ray experiments see Engelman and Rothman (1972) and Finean (1990).

The present work is an outgrowth of the recent finding that "condensed complexes" of cholesterol and phospholipids can model a number of unusual physical properties of these mixtures in monolayers at the air-water interface (Radhakrishnan and McConnell, 1999a, b). These properties include 1) phase diagrams with pairs of upper miscibility critical points (Radhakrishnan and McConnell, 1999b), 2) a large response to electric field gradients in membranes having the complex stoichiometry (Radhakrishnan and McConnell, 1999c), and 3) a rapid increase in the cholesterol chemical potential at the complex stoichiometry (Radhakrishnan and McConnell, 2000). In essence, the model is one in which the interactions between cholesterol and phospholipids are treated as reversible chemical reactions. The present work was undertaken to test the adequacy

of this model when applied to data from the scanning calorimetry of bilayer mixtures of cholesterol and phospholipid. In this work, two special assumptions have been made: it is assumed that only a single complex is formed between cholesterol and phospholipid, and it is assumed that the broad heat absorption seen in the scanning calorimetry is due to thermal dissociation of this complex.

THERMODYNAMIC MODEL

In this study the large deviations from ideality in cholesterol-phospholipid mixtures are attributed to the formation of a single complex of cholesterol and phospholipid. Our calculations use a regular solution model for mixtures of complex, cholesterol, and phospholipid molecules. This model has been described earlier in the context of lipid monolayers at room temperature and variable surface pressure (Radhakrishnan and McConnell, 1999b). Here we use the same model, except that temperature rather than pressure is an independent variable.

The reversible chemical reaction for the formation of condensed complexes is

$$nqC + npP \rightleftharpoons C_{nq}P_{np} \qquad (1)$$
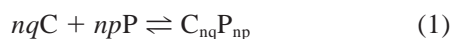
where p and q are relatively prime integers used to define the relative stoichiometric composition, and n is an oligomerization number that reflects the cooperativity of complex formation. The use of separate parameters for stoichiometry and cooperativity facilitates fitting the model to experimental data. If N_0 molecules of cholesterol and phospholipid are initially present (before reaction) and the initial cholesterol mole fraction is X_{C0}, the amounts of free cholesterol (N_C), free phospholipid (N_P), and complex (N_X) present in the sample following complex formation may be expressed in terms of an extent of reaction variable, ξ,

$$N_C = N_0(X_{C0} - nq\xi)$$
$$N_P = N_0(1 - X_{C0} - np\xi)$$
$$N_X = N_0\xi \qquad (2)$$

The total number of molecules in the reacted sample is the sum of these,

$$N = N_0(1 + (1 - nq - np)\xi) \qquad (3)$$

Using regular solution theory, the free energy G and enthalpy H of the mixture of cholesterol, phospholipid, and complex are

$$G = \sum_i N_i H_i^\theta + Nk_B T \sum_i X_i \ln X_i + N \sum_{i<j} \alpha_{ij} X_i X_j \quad (4)$$

Here the X_i are the mole fractions of the species, $X_i = N_i/N$. The use of $\ln X$ terms to represent the entropy of mixing is clearly a crude approximation in light of the large molecular size of the complex. However, absent knowledge of the

TABLE 1 Reference chemical potentials and standard enthalpies

Species	μ_i^θ	H_i^θ
Cholesterol	0	0
Phospholipid (l)	0	ΔH_m
Phospholipid (s)	$\Delta H_m(T - T_m)/T_m$	0
Complex	$-k_B \ln K_{eq}$	$np\Delta H_m + \Delta H_{rxn}$

structure of the complex, a more detailed treatment is not warranted. For a discussion of a related problem, see Corrales and Wheeler (1989a).

In Eqs. 4 and 5, the α_{ij} are pairwise interaction terms for the free cholesterol, free phospholipid, and complex, and are related to the respective (binary mixture) critical temperatures by

$$\alpha_{ij} = 2k_B T_{ij} \qquad (6)$$

The reference chemical potentials μ_i^θ and standard enthalpies H_i^θ for cholesterol, the liquid (l) and solid (s) states of the phospholipid, and the complex, are given in Table 1. In these expressions, ΔH_m is the heat of melting of the pure solid phospholipid phase, and ΔH_{rxn} is the heat of reaction corresponding to Eq. 1. In this work the heat of reaction is negative, indicating that complex formation is exothermic. K_{eq} is the equilibrium constant for the reaction, which in the case of ideal mixing of cholesterol, phospholipid, and complex may be expressed as

$$K_{eq} = \frac{X_{complex}}{X_c^{nq} X_P^{np}} \qquad (7)$$

If the mixing is non-ideal, the equilibrium constant is equal to the corresponding ratio of chemical activities. The chemical activity of species i is $\exp(\mu_i/k_B T)$, where the chemical potential μ_i is $\partial G/\partial N_i$.

The enthalpy and entropy of reaction are assumed to be essentially constant over the temperature range of interest. As a result, the temperature dependence of the equilibrium constant is

$$K_{eq} = K_{eq}^\theta \exp\left[\frac{\Delta H_{rxn}}{k_B}\left(\frac{1}{T^\theta} - \frac{1}{T}\right)\right] \qquad (8)$$

The reference temperature T^θ is room temperature, 300 K.

For a particular initial composition X_{C0} and temperature T, the free energy in Eq. 4 is minimized with respect to the extent of reaction ξ to find the equilibrium extent of reaction, ξ_{eq}. Alternatively, Eq. 7 (or its equivalent using chemical activities) may be solved in conjunction with Eqs. 2; this method was used for calculations involving ideal reaction mixtures. The extent of reaction at equilibrium is then used for calculations of the equilibrium composition and enthalpy. The relationships between the equilibrium extent of reaction and sample composition and temperature in an ideal reaction mixture are illustrated in Figs. 1 and 2 A for
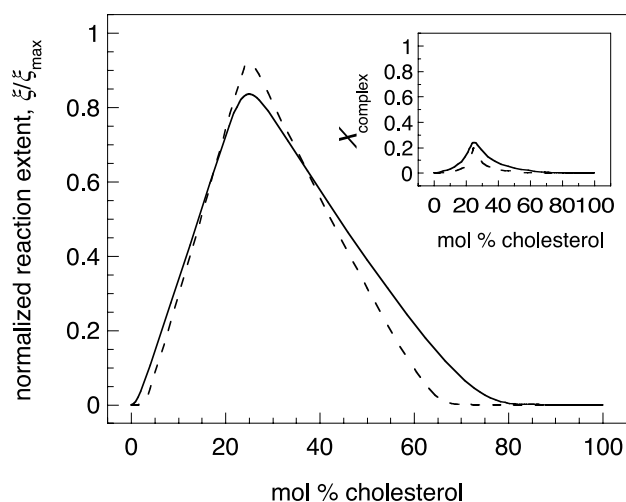
FIGURE 1 Variation of the equilibrium reaction extent with respect to (initial) cholesterol composition in an ideal solution for a 3:1 complex with a cooperativity of $n = 4$ (*solid line*) and 12 (*dashed line*) and a normalized equilibrium constant of $\hat{K}_{eq} = 20$. The extent of reaction ξ has been normalized with respect to the maximum extent at the stoichiometric composition, ξ_{max}, as described in the text. *Inset*: the mole fraction of complex versus composition. The solid-liquid transition of the phospholipid was not included in these calculations.

reactions with a 3:1 stoichiometry and cooperativity values of $n = 4$ and $n = 12$. For illustrative purposes, the extents of reaction are normalized with respect to the maximum possible extent at the stoichiometric composition, ξ_{max}. This normalized extent corresponds to the fraction of molecules in the sample that have reacted to form complex. An alternative measure of the extent of reaction is the mole fraction of complex in the equilibrium mixture; this is shown in the inset to Fig. 1.

In the event that a plot of G_{eq} vs. X_{C0} shows that the free energy of the sample can be reduced by phase separation, a double tangent construction is used to determine the compositions of the two coexisting phases. The foregoing thermodynamics are then applied to each phase. For calculations of solid-liquid coexistence, Eq. 4 was used for the free energy of the liquid phase; the solid phase was taken to be pure phospholipid ($X_C = 0$), with a free energy of $N\mu_{P(s)}^{\theta}$. As discussed later, only a very limited region of liquid-liquid coexistence—or no such coexistence at all—is found with the parameter sets that best fit the experimental data. Accordingly, most of the calculations described in the present study do not involve liquid-liquid phase separation.

For calculations of DSC curves and their associated thermodynamic parameters, the heat capacity of the mixture was determined by numerical differentiation of the calculated enthalpy using the relation $C_P = (\partial H/\partial T)_P$. To avoid singularities in the heat capacity, for example at phase boundaries, enthalpy values were calculated at small temperature intervals over the range of interest, and exponential smoothing was applied to these values before numeric dif-

ferentiation. Because the heat capacities of the pure cholesterol and solid and liquid phospholipid are neglected, the result is an excess heat capacity as measured in DSC experiments. It may be noted that in the simplified model used here, the heat capacity of the complex is taken to be the same as the free cholesterol and phospholipid; this is implicit in the assumption that the ΔH of complex formation is independent of the temperature.

The broad component of the DSC heat absorption is attributed to the thermal reversal of the exothermic reaction Eq. 1 (Fig. 2 *A*). Illustrative calculations of this contribution to the heat capacity for two different values of the cooperativity are shown in Fig. 2 *B*. The heat absorptions shown are calculated for ideal mixtures having the stoichiometric composition. For convenience, the temperature of the maxima in these heat absorption curves is referred to hereafter as the *dissociation temperature* of the complex, T_d. At this temperature, indicated in Fig. 2, *A* and *B* by small squares, the extent of reaction is changing most rapidly with temperature. In general, the position of this maximum varies with the composition of the sample. Except as otherwise noted, T_d refers to the heat absorption peak at the stoichiometric composition.

As Fig. 2 *B* shows, the calculated heat absorption curves are asymmetric. They are not well represented by Gaussian peak functions. To fit the calculated curves, we instead used generalized exponential peak functions (Vaidya and Hester, 1984). Where phospholipid melting and complex decomposition occur, a linear combination of these peak functions was used to fit the calculated curves. The transition temperatures, enthalpies, and half-widths reported here were calculated on the basis of these best-fit peak functions.

An important result is the finding that the half-width of the calculated heat absorption curve for complex decomposition depends strongly on the cooperativity parameter n of the reaction, but only weakly on the standard equilibrium constant K^θ; this is illustrated in Fig. 2 *C*. This result provides a means of estimating the reaction cooperativity from the experimental data, as discussed later.

Fig. 3 *A* shows the calculated heat capacity profile for an ideal reaction mixture as a function of the cholesterol content of the bilayer. Note that the temperature maximum of the profile increases as the stoichiometric composition is approached. In an ideal solution, but not necessarily in a regular solution, this temperature then decreases with increasing cholesterol concentration. This trend is illustrated in Fig. 3 *B*. The transition enthalpy, obtained by integration under the heat capacity curve, reaches a maximum at the stoichiometric composition and decreases for larger concentrations of cholesterol, as shown in Fig. 3 *C*. This plot is idealized inasmuch as it assumes that the heat capacity is integrated over an infinite temperature range. It is seen in Fig. 3 *A* that the transition peak becomes narrower near the stoichiometric composition; this effect is shown in the plot of $\Delta T_{1/2}$ versus composition in Fig. 3 *D*.
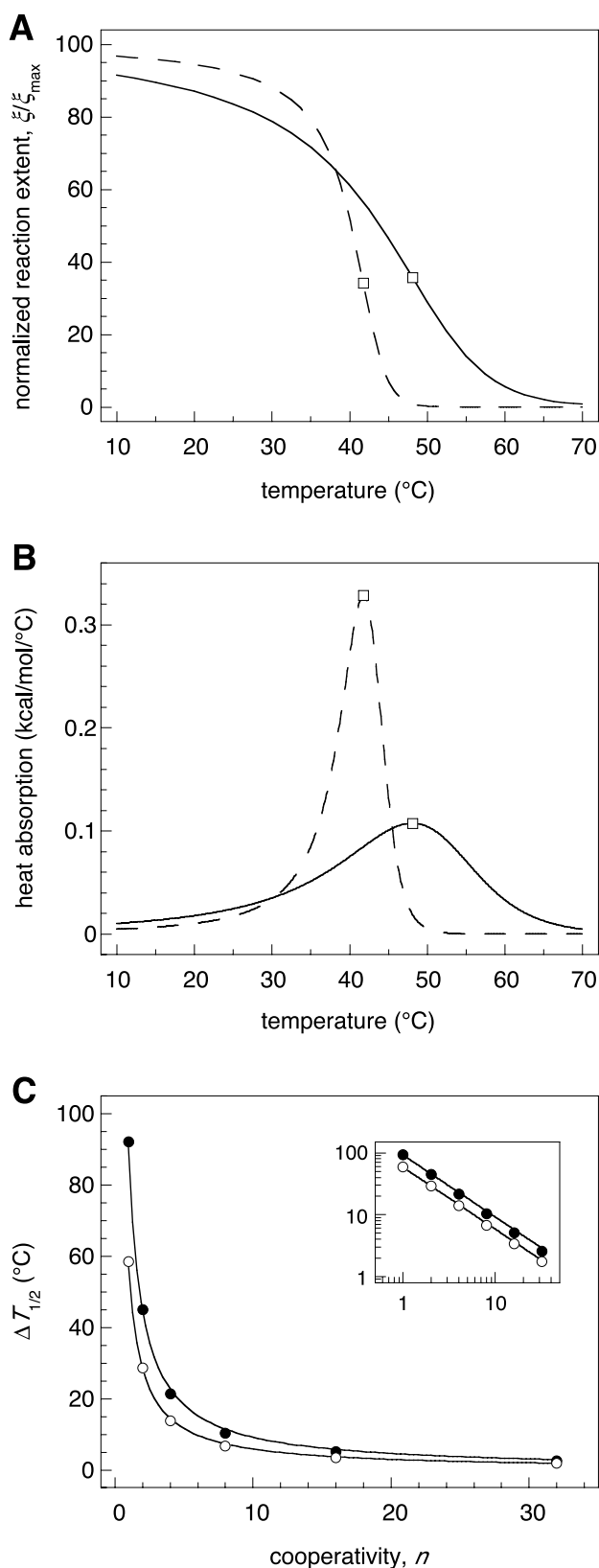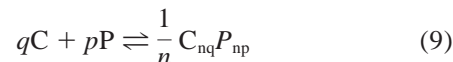
CHOICE OF PARAMETERS

In discussing the reaction parameters it is useful to introduce a normalized form of the reaction in Eq. 1,

$$qC + pP \rightleftharpoons \frac{1}{n} C_{nq}P_{np} \qquad (9)$$

This normalized form of the reaction is described by the thermodynamic parameters $\Delta \hat{H}_{rxn}$ and $\hat{K}_{eq}$, which are related to the enthalpy and equilibrium constant of reaction (1) by

$$\Delta H_{rxn} = n\Delta \hat{H}_{rxn}$$

$$K_{eq} = (\hat{K}_{eq})^n \qquad (10)$$

Use of these normalized parameters allows the cooperativity of complex formation to be adjusted independently of the total enthalpy associated with complex decomposition and, to some extent, the decomposition temperature of the reaction.

The parameters used in the illustrative ideal-solution calculations described above are similar to those used in the calculations to fit the experimental results (Table 2). In these more detailed calculations, the parameters include the melting temperatures T_m and heats of melting ΔH_m taken from the literature for DMPC, DPPC, DSPC, and DAPC (Marsh, 1990). Parameters relating to the chemical reaction described by Eq. 1 were determined from the experimental DSC data. These parameters include the stoichiometric coefficients p and q, the normalized heat of reaction $\Delta \hat{H}_{rxn}$, the standard normalized equilibrium constant $\hat{K}_{eq}^\theta$, and the cooperativity n. The coefficients p and q are determined from the stoichiometric composition, at which the enthalpy of the broad heat absorption peak is a maximum. The normalized heat of reaction is related to the integrated heat absorption of the broad peak at the stoichiometric composition by $\Delta \hat{H}_{rxn} = p(H_{broad})$ with a small empirical correction for systematic errors in the curve-fitting procedure.

Once the normalized heat of reaction has been determined, the standard normalized equilibrium constant is chosen to give a decomposition temperature T_d that agrees with the observed temperature of the broad transition peak at the stoichiometric composition. As discussed later, the cooperativity parameter n is chosen to give broad transition half-widths in agreement with the experimental values. Each of

FIGURE 2 Thermal decomposition of a 3:1 complex with a cooperativity of $n = 4$ (*solid lines*) or 12 (*dashed lines*), a standard normalized equilibrium constant of $\hat{K}_{eq}^\theta = 20$ and a normalized heat of reaction $\Delta \hat{H}_{rxn} = -12$ kcal/mol. (*A*) Normalized extent of reaction at the stoichiometric composition versus temperature. The decomposition temperature T_d for each reaction is indicated by an empty square. (*B*) Heat absorption versus temperature for the decompositions shown in (*A*). (*C*) Half-width of the decomposition transition at the stoichiometric composition for various values of n, with standard normalized equilibrium constants of 20 (*filled circles*) and 0.2 (*open circles*). The points were fit to hyperbolic curves, $y = c/x$ (*solid lines*). *Inset*: a log-log plot of the same points. For these calculations, ideal mixing was assumed, and the solid-liquid transition of the phospholipid was not included.
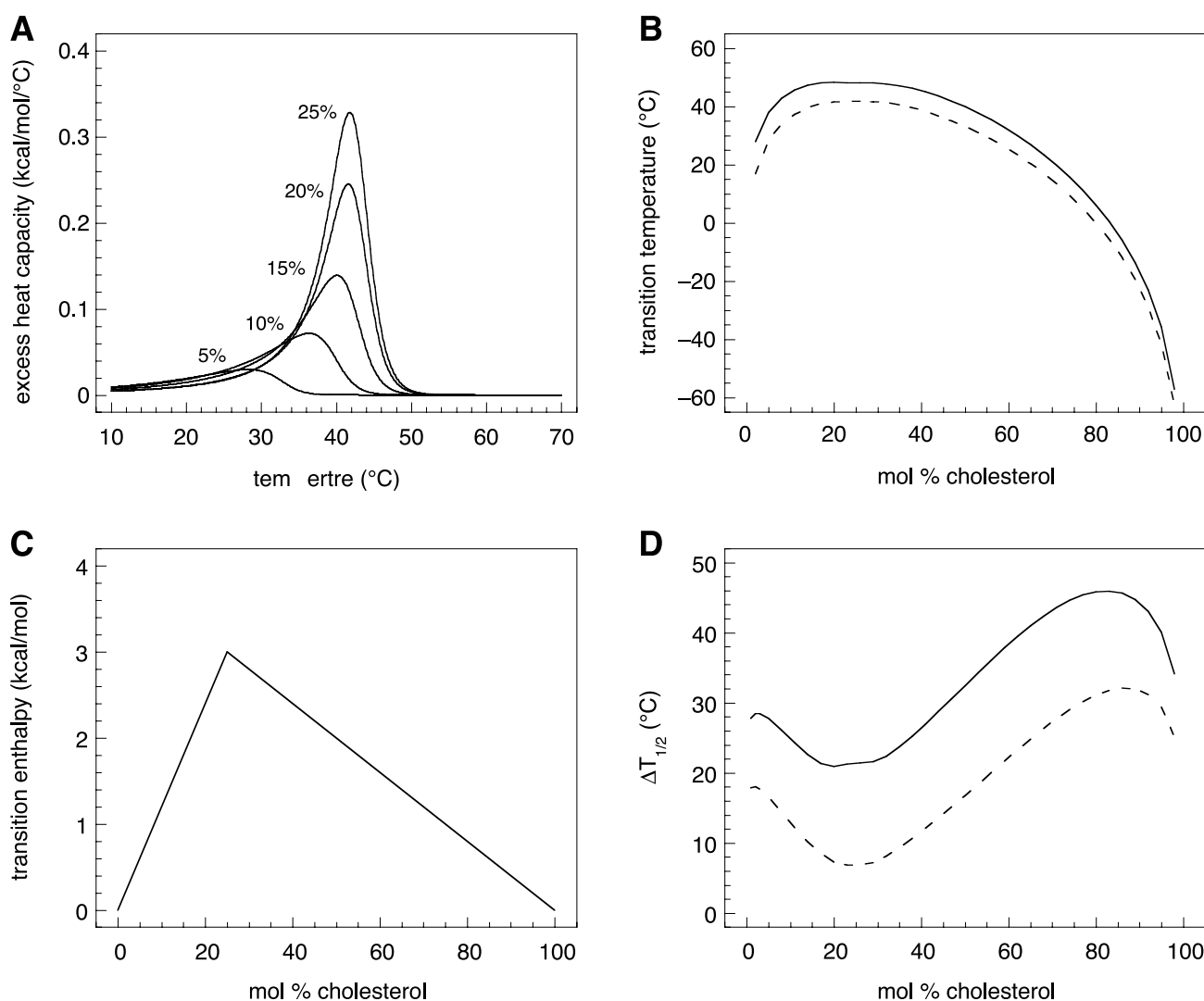
FIGURE 3   Variation of the temperature and half-width of the decomposition transition with composition; reaction parameters are the same as in Fig. 2 (*A*) Heat absorption curves for the $n = 4$ reaction at compositions of 5, 10, 15, 20, and 25 mol % cholesterol. (*B*) Transition temperature as a function of composition for $n = 4$ (*solid line*) and 12 (*dashed line*). The stoichiometric composition is 25 mol % cholesterol. (*C*) Enthalpy of the decomposition transition versus composition; this curve is the same for both $n = 4$ and 12. (*D*) Half-width of the decomposition transition versus composition for $n = 4$ (*solid line*) and 12 (*dashed line*). For these calculations ideal mixing was assumed, and the solid-liquid transition of the phospholipid was not included.

the four phospholipids was assumed to have the same reaction stoichiometry and cooperativity. The stoichiometric parameters chosen, $q = 1$ and $p = 3$, corresponding to a complex containing 25 mol % cholesterol, are also similar

TABLE 2   Parameters used to fit the experimental data, with the corresponding decomposition temperatures

Phospholipid	Chain Length	T_m (°C)	ΔH_m (kcal/mol)	$\Delta \hat{H}_{rxn}$ (kcal/mol)	$\hat{K}^{\theta}_{eq}$	T_d (°C)
DMPC	14	23	6	−6.3	5.7	32
DPPC	16	41	8	−9.6	11	42
DSPC	18	55	10	−13.2	31	53
DAPC	20	66	12	−19.8	208	63

to the values used in monolayer studies (Radhakrishnan and McConnell, 1999b).

The only parameters in the model that are not readily determined from the experimental data are the regular solution interaction parameters α_{PC}, α_{PX}, and α_{CX}. The experimental data do place constraints on the values of these parameters. In general, the values considered are of the same order of magnitude as those used in earlier simulations of monolayer phase diagrams. The α values are in the range of 0.5 to 3 $k_B T^{\theta}$ (Anderson and McConnell, 2000). However, the parameters for monolayers are pressure-dependent, and it is not straightforward to make a direct comparison between monolayers and bilayers in this respect. For simplicity, the same set of interaction terms was used for all four phospholipids.
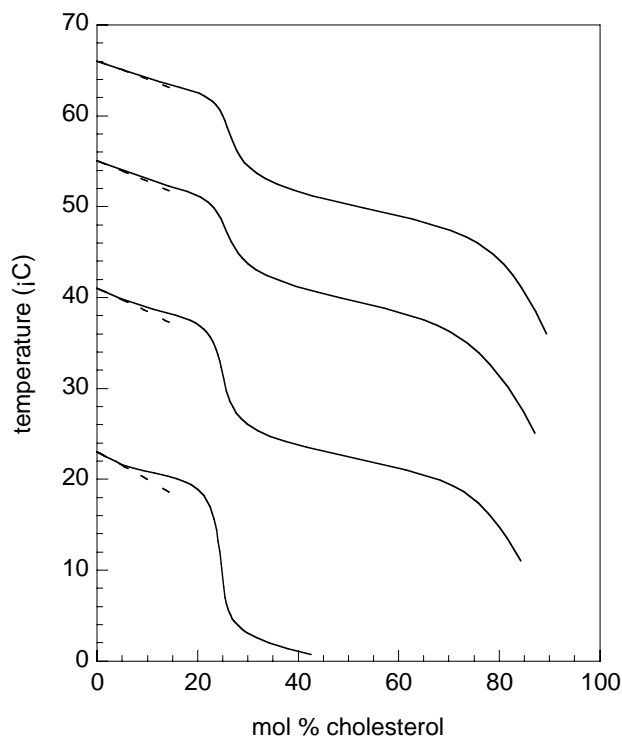
FIGURE 4 Calculated temperature/composition phase diagrams for regular solutions of cholesterol with saturated phospholipids having chain lengths of (*bottom* to *top*) 14 (DMPC), 16 (DPPC), 18 (DSPC), and 20 (DAPC). In each case the phospholipid is taken to form a 3:1 complex with cholesterol. The dotted lines indicate ideal-solution melting point depressions for low cholesterol compositions. Parameters used for all chain lengths: $p = 3$; $q = 1$; $n = 12$; $T_{CP} = 100$ K; $T_{CX} = 400$ K; $T_{PX} = 100$ K. Chain length-dependent parameters are given in Table 2.

The general approach used in fitting to the experimental data is to extract values for the model parameters from some of the experimental results and then test the model by comparison of predictions with other observations. A potential major flaw in such comparisons stems from the difficulty of deconvoluting the experimental overlapping sharp and broad peaks in the heat capacity profiles. In our calculations the individual peaks are not symmetric. McMullen et al. have presumably used a deconvolution based on symmetric Gaussian peak shape functions (McMullen et al., 1993). The reader must refer to their work to make detailed comparisons between our calculated results and the DSC measurements.

RESULTS

Phase diagrams and DSC curves

Calculated phase diagrams corresponding to mixtures of cholesterol with DMPC, DPPC, DSPC, and DAPC are shown in Fig. 4; the parameters used are given in the figure legend and in Table 2. DSC curves for mixtures of DPPC with various cholesterol composition are shown in Fig. 5. In each of the phase diagrams there is a region of solid-liquid
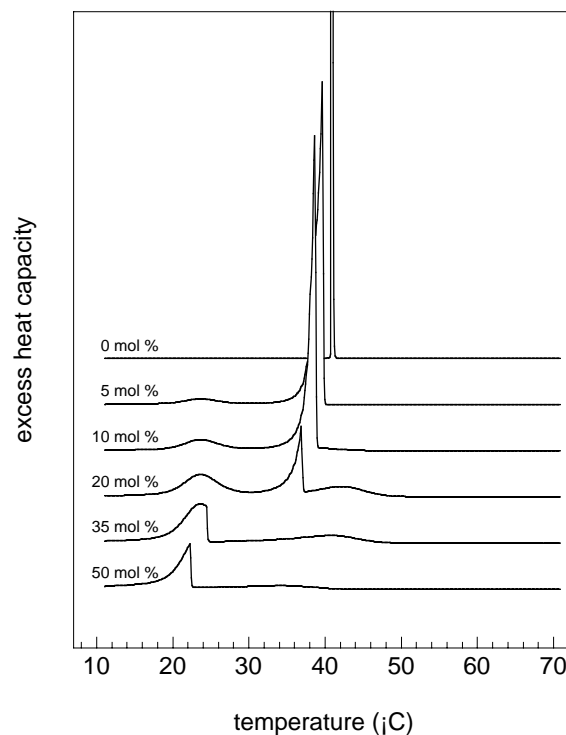

FIGURE 5 Calculated DSC curves for the DPPC/cholesterol mixtures described in Fig. 4 at various cholesterol compositions.

coexistence that can be subdivided into high- and low-temperature regions. In each case the region of coexistence near the T_m of the phospholipid disappears rather abruptly for cholesterol compositions exceeding the stoichiometric fraction, $q/(p + q) = 0.25$. At lower temperatures, the region of solid-liquid coexistence extends to higher cholesterol concentrations. This extension of the coexistence region of the phase diagrams, referred to here as the "foot," gives rise to the spurious low-temperature heat absorption peaks shown in Fig. 5. For example, the calculated DSC curves for 20% cholesterol in Fig. 5 shows three well-defined heat absorption peaks: the highest-temperature peak is due to the dissociation of the complex, the central peak is due to the chain melting transition, and the lowest-temperature peak is also due to chain melting and is related to the spurious foot in the phase diagram.

The foot in each of the phase diagrams in Fig. 4, and the corresponding spurious low-temperature heat capacity peaks seen in Fig. 5, are an intrinsic property of the condensed complex model, provided that 1) the heat of reaction between *solid* phospholipid and cholesterol is endothermic, and 2) only a single complex with a given n is included in the model. Larger heats of reaction yield diagrams where there is less appearance of solid-liquid coexistence beyond the stoichiometric composition. Diagrams of this type are illustrated in Fig. 6. Importantly, the heat capacities of solid and liquid phospholipid bilayers are nearly the same (Marsh, 1990). This means that the heat of reaction between
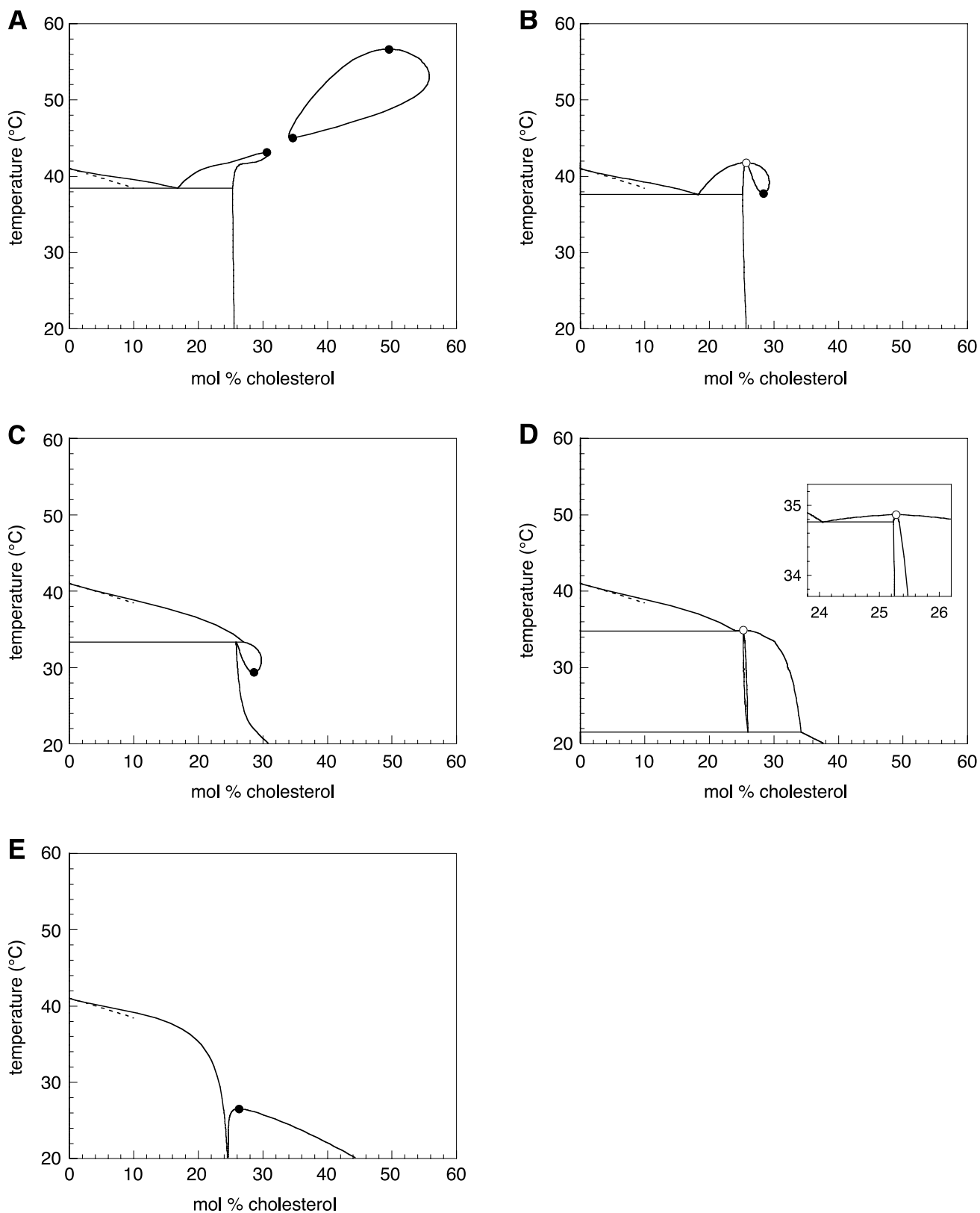
FIGURE 6   Representative sample of calculated cholesterol/DPPC phase diagrams showing a liquid-liquid coexistence region. In all cases, $T_m = 41°C$, $\Delta H_m = 8$ kcal/mol, and the reaction stoichiometry is $p = 3$, $q = 1$, with a cooperativity of $n = 4$. Black dots indicate miscibility critical points; open circles indicate critical areatrope points, as discussed in the text. (A) Phospholipid-cholesterol immiscibility. $T_{CP} = 330$ K; $T_{CX} = 300$ K; $T_{PX} = 500$ K; $\Delta H_{rxn} = -20$ kcal/mol; $\hat{K}_{eq}^{\theta} = 16$. The decomposition temperature is $T_d = 44.9°C$. (B) Miscible phospholipid-cholesterol. $T_{CP} = 100$ K; $T_{CX} = 200$ K; $T_{PX} = 500$

solid phospholipid and cholesterol at temperatures below T_m is equal to the sum of the heat of reaction for the liquid phospholipid plus cholesterol and the heat of melting of the solid phospholipid.

None of the phase diagrams in Fig. 4 shows liquid-liquid immiscibility. The diagrams in Fig. 6 illustrate such immiscibilities. The inclusion of parameters yielding these immiscibilities does not improve agreement with any of the various experimental results, except for the cholesterol dependence of the shift of the broad transition, where the improvement is marginal. However, only a very limited region of liquid-liquid coexistence involving the complex at higher temperatures is consistent with the present analysis of the DSC results, for reasons discussed later. The calculations described below use the parameters corresponding to Fig. 4, which do not give liquid-liquid immiscibility.

Illustrative heat absorption curves corresponding to calculations of the DPPC-cholesterol mixture described above are shown in Fig. 5. The sharp heat absorption transition due to phospholipid melting becomes weaker and appears at a lower temperature upon addition of cholesterol, disappearing altogether at a composition of ~25% cholesterol. A second, broader transition is visible at a higher temperature at 10% cholesterol. This transition grows larger as the cholesterol composition is increased, reaching a maximum near 25% cholesterol, after which it becomes smaller again. As noted above, there is a spurious heat absorption at the lower temperatures.

Effect of cholesterol on the main phase transition

Fig. 7 *A* gives the calculated decrease in temperature of the sharp chain melting transition as a function of cholesterol concentration. This decrease in melting temperature reflects the upper boundary of the solid-liquid two-phase region in the phase diagrams in Fig. 4. It will be noted that at low cholesterol concentrations the decrease in melting temperature is close to the ideal solution limit in the absence of complex (*dotted lines* in Fig. 4). As discussed later, the experimental and model main chain melting temperatures are equal to within 1–2°C at higher cholesterol concentrations (15%). Calculated enthalpy changes associated with the sharp transition are given in Fig. 7 *B*. These calculated values are in good agreement with experiment. This is not a strong test of the model, however, because the reaction stoichiometry is set by the zero of the observed sharp heat capacity curve.

Parameters of the broad transition

McMullen et al. (1993) have analyzed the broad heat capacity profile with respect to its peak position ("net temperature shift," δT_{broad}), the integral under the broad component of the heat capacity curve (enthalpy, H_{broad}), and the half-width of the peak, $\Delta T_{1/2}$. Calculations of these are shown in Fig. 7, *C–E* as a function of composition. The calculated enthalpy for the broad transition has a maximum at the putative stoichiometric composition. The reported maxima in the transition enthalpies are in the range of 20–25% cholesterol.

Calculated shifts δT_{broad} are given in Fig. 7 *C*. The experimental work of McMullen et al. (1993) shows both positive and negative variations in the temperature shifts of the broad components as a function of cholesterol concentration. Here we only consider data for cholesterol concentrations above 20 mol %, because below that concentration the shifts are small and there is doubtless strong overlap with the heat absorption due to the main transition. Above 20% some experimental shifts are to higher temperatures (e.g., 13:0, 14:0, 15:0), some shifts are very small (<2°C), (e.g., 16:0, 17:0, 18:0); whereas some shifts are to lower temperatures (19:0, 20:0, 21:0). Our calculations generally show a decrease in this heat absorption temperature at higher cholesterol compositions (Fig. 3 *B*). This is the second instance where there is a qualitative difference between calculated and experimental results. The introduction of mean-field non-ideal mixing (liquid-liquid immiscibility) can ameliorate this problem, but not remove it. It may be noted that the value of the cooperativity parameter n has very little effect on the shape of the δT_{broad} vs. X_{chol} and ΔH_{broad} vs. X_{chol} curves.

Calculated half-widths $\Delta T_{1/2}$ are given in Fig. 7 *E*. Above 20% cholesterol the observed and calculated widths of the broad transition increase with increasing cholesterol concentration. Below this cholesterol concentration there is some non-monotonic variation in the calculated widths, but this variation might easily be lost in the deconvolution of experimental data.

DISCUSSION

The condensed complex model used here to interpret the calorimetry of cholesterol-phospholipid mixtures in bilayers is closely related to the model used earlier to describe these mixtures in monolayers at the air-water

---

K; $\Delta H_{rxn} = -14$ kcal/mol; $\hat{K}_{eq}^{\theta} = 28$. The decomposition temperature is $T_d = 45.4$°C. (*C*) Low decomposition temperature. $T_{CP} = 100$ K; $T_{CX} = 200$ K; $T_{PX} = 500$ K; $\Delta H_{rxn} = -15.6$ kcal/mol; $\hat{K}_{eq}^{\theta} = 15.8$. The decomposition temperature is $T_d = 36.5$°C. (*D*) $T_{CP} = 100$ K; $T_{CX} = 300$ K; $T_{PX} = 500$ K; $\Delta H_{rxn} = -13.2$ kcal/mol; $\hat{K}_{eq}^{\theta} = 15.4$. The decomposition temperature is $T_d = 37.2$°C. (*E*) Complex-cholesterol immiscibility. $T_{CP} = 100$ K; $T_{CX} = 400$ K; $T_{PX} = 100$ K; $\Delta H_{rxn} = -28$ kcal/mol; $\hat{K}_{eq}^{\theta} = 56$. The decomposition temperature is $T_d = 43.2$°C. For clarity, these phase diagrams use a cooperativity of $n = 4$ rather than the preferred $n = 12$. Increasing the cooperativity increases the sharpness of the various features without introducing or removing any of the two-phase regions.
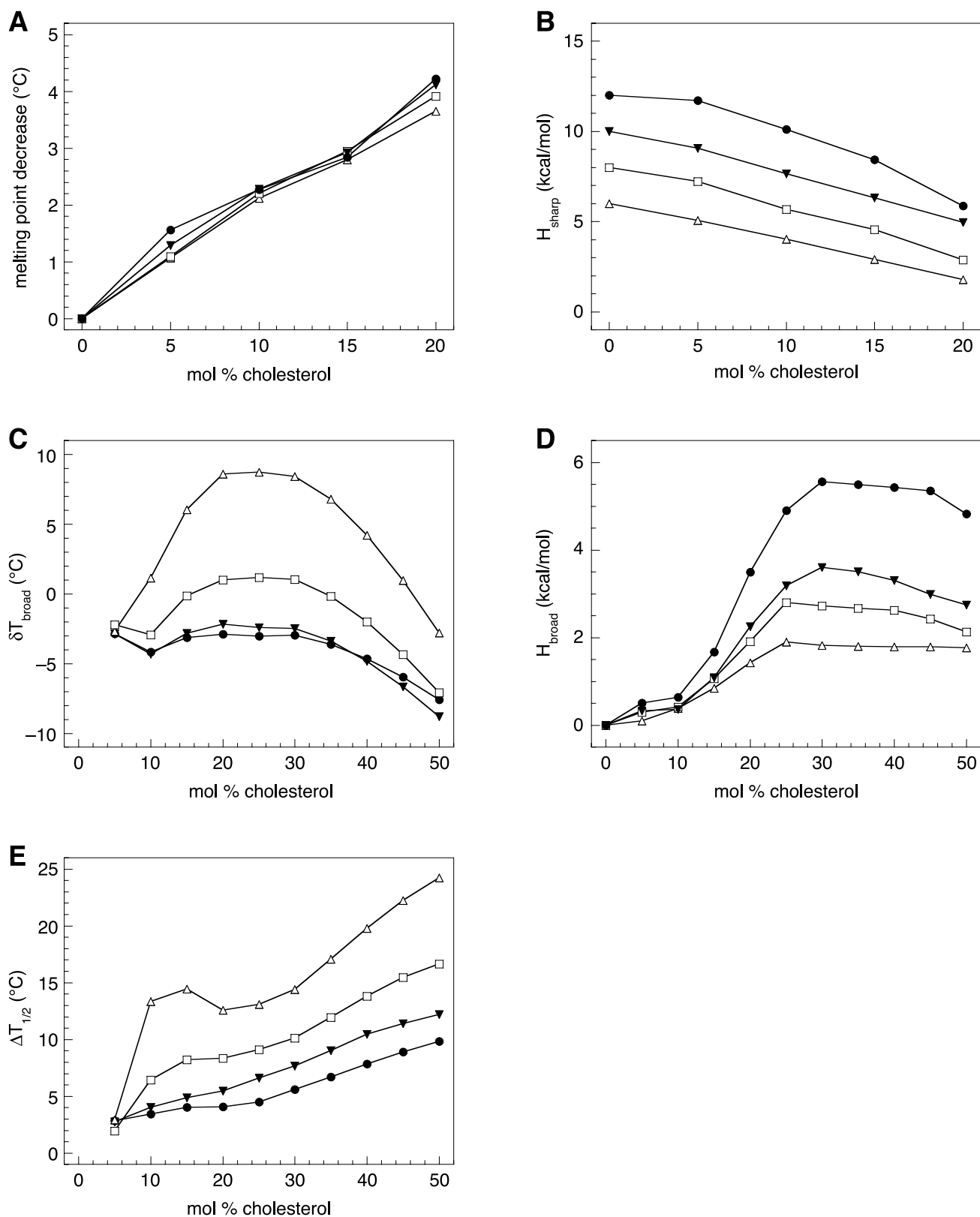
FIGURE 7 Trends in the calculated transition parameters for the sharp and broad transitions with respect to composition for mixtures of cholesterol with saturated phosphatidylcholines of chain length 14 (DMPC, *open triangles*), 16 (DPPC, *open squares*), 18 (DSPC, *filled inverted triangles*), and 20 (DAPC, *filled circles*), whose phase diagrams are shown in Fig. 4. (*A*) Decrease in the sharp (melting) transition temperature versus cholesterol composition. (*B*) Enthalpy of the sharp transition. (*C*) Change in the broad (decomposition) transition temperature relative to T_m. (*D*) Enthalpy of the broad transition. (*E*) Half-width of the broad transition. In all calculations the parameters used are the same as in Fig. 4.

interface (Radhakrishnan and McConnell, 1999b). The model assumes that interactions between cholesterol and phospholipids can be represented by reversible chemical reactions. Two special, more restrictive assumptions are also made. It is assumed that only one complex is formed, and it is assumed that the thermal dissociation of this complex is responsible for the broad heat absorption. This application of the model to bilayers involves other assumptions that are also distinct from the work of other laboratories. For example, we assume that cholesterol and complex have a negligible solubility in the solid phases of the phosphatidylcholines studied. Other investigators have inferred that the cholesterol solubility is substantial (Ipsen et al., 1987; Vist and Davis, 1989). Note that at low cholesterol concentrations ($\leq$10 mol %) where there is very little complex, the melting point depression follows near-ideal behavior. Therefore, there cannot be a high solubility of cholesterol in the solid phase. We have assumed throughout that the transbilayer coupling is such that opposite sides of the bilayer are equivalent. Quite recent work has provided evidence for this assumption (Dietrich et al., 2001). These investigators have shown that in specific mixtures of phospholipids and cholesterol, coexisting liquid phases are formed that appear to have inside-outside symmetry.

Both the experimental and classical ideal freezing point depressions at 5% cholesterol (no complex) are ~1°C. In the range 10–15% cholesterol the calculated depressions are ~1° too large. The calculated melting points in this composition range are elevated with respect to the classical ideal-solution values. Deviations from the classical ideal melting temperature can arise from repulsive cholesterol-phospholipid interactions. In general, for a pure solid phospholipid coexisting with a regular solution whose free energy is described by Eq. 4, the melting point depression is described by

$$\delta T_\mathrm{m} = \frac{T_\mathrm{m}^\circ(\alpha_\mathrm{PC}X_\mathrm{C}^2 + k_\mathrm{B}T_\mathrm{m}^\circ\ln[1 - X_\mathrm{C}])}{\Delta H_\mathrm{m} - k_\mathrm{B}T_\mathrm{m}^\circ\ln[1 - X_\mathrm{C}]} \quad (11)$$

When $\alpha_\mathrm{PC} = 0$, Eq. 11 describes the ideal-solution melting point depression. Importantly, at low cholesterol concentrations effects involving the complex do not contribute significantly to the melting point depression in these calculations because 1) very little complex is formed at low cholesterol concentrations due to the cooperativity of complex formation, and 2) the complex decomposition temperature is near the phospholipid chain melting temperature.

A second difference relative to other work concerns the origin of the broad heat absorption. In the work of Ipsen et al., this is attributed to melting associated with a monotectic point (Ipsen et al., 1989). Monotectic points are found in the phase diagrams illustrated in Fig. 6, *A* and *B*. McMullen et al. (1993) have described the broad heat absorption as being due to "melting of the cholesterol-rich phosphatidylcholine domains," whereas here we interpret the broad heat absorp-

tion as being due to the thermal dissociation of the condensed complexes.

Still another difference between the present model and previous work relates to liquid-liquid immiscibility. A number of studies have proposed the formation of immiscible liquids in cholesterol-phospholipid bilayers (Rechtenwald and McConnell, 1981; Ipsen et al., 1987). At present there is no compelling experimental evidence for this immiscibility for the particular mixtures studied here, although there is abundant evidence for this immiscibility in monolayers (McConnell, 1991), and also in bilayers with other lipid compositions (Dietrich et al., 2001). The model parameters we use limit the temperature range for possible liquid-liquid immiscibility involving the complex. This limitation is related to the position of the peak of the broad heat absorption. It will be seen, for example, in Fig. 1 that the concentration of complex decreases sharply near the dissociation temperature of the complex. For most (but not all) of the phospholipids studied experimentally, the inferred complex melting temperature is close to the melting temperature of the solid (see Fig. 8 in McMullen et al., 1993 for 25% cholesterol concentration). Therefore, there is little complex present above the chain melting transition temperature, so there cannot be a large region of immiscibility of complex and a second liquid above the chain melting transition temperature. In monolayers containing different individual phospholipids, immiscibility arises from a combination of cholesterol-phospholipid repulsions, phospholipid-complex repulsions, and complex-cholesterol repulsions (Radhakrishnan and McConnell, 1999a).

The calculated phase diagrams shown in Fig. 6 illustrate the types of liquid-liquid immiscibilities that in principle can arise, using parameters that are roughly compatible with the DSC data. These calculations use mean field repulsions between the various components. Some of these same repulsions are described as giving rise to the various observed immiscibilities in monolayers at room temperature and lower monolayer pressures. In monolayers the applied pressure serves to increase or decrease the critical temperatures. Some of the interaction parameters used for Fig. 6 are of the same order of magnitude as those used for the monolayers, typical values of which are equivalent to critical temperatures of $T_\mathrm{CP} \approx 550$ K, $T_\mathrm{CX} \approx 750$ K, $T_\mathrm{PX} \approx 450$ K (Anderson and McConnell, 2000). The higher temperature immiscibility region in Fig. 6 *A* arises from an assumed strong repulsion between phospholipid and cholesterol in this case; black dots refer to critical points. The white dots in Fig. 6 *B* and *D* are *areatropes*, and represent a first-order liquid-liquid phase transition in which the concentration of complex changes discontinuously (Corrales and Wheeler, 1989b). The interaction parameters used for Fig. 6 *E* are the same as those in Fig. 4; however, the standard equilibrium constant and heat of reaction are significantly larger. The correspondingly greater stability of the complex gives rise to cholesterol-complex immiscibility in this case. The as-
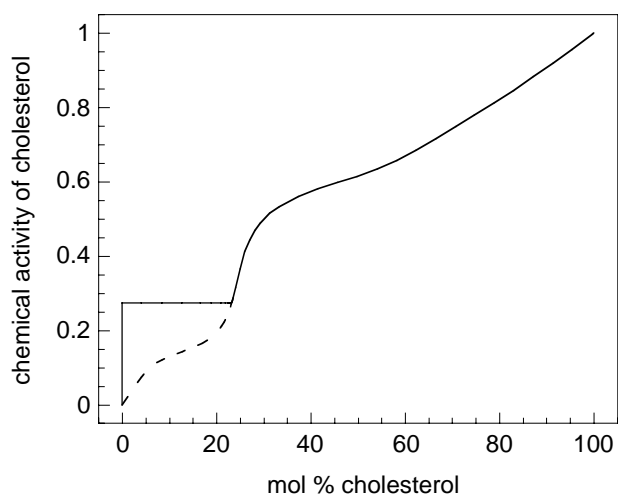
FIGURE 8 Chemical activity of cholesterol in a mixture with DPPC corresponding to the phase diagram in Fig. 4, at a temperature of 35°C. The dotted line indicates the cholesterol activity if the DPPC solid/liquid transition is omitted from the calculation.

sumed larger heats of reaction also eliminate the foot in each of the phase diagrams in Fig. 6. These larger heats of reaction are not compatible with the reported heat absorptions (McMullen et al., 1993).

Previous work from other laboratories described a "liquid-ordered phase" for mixtures of cholesterol and phospholipids (Ipsen et al., 1987; Vist and Davis, 1989; Nielsen et al., 2000). This phase corresponds to the temperature-composition region in Fig. 4 at cholesterol concentrations above 25 mol %. This phase is described as the higher cholesterol liquid region of the phase diagram, the region forming the higher cholesterol phase boundaries of the solid-liquid and putative liquid-liquid two-phase regions. This picture is consistent with our model in that the higher cholesterol regions of our phase diagrams could be a miscible mixture of cholesterol and complex. *The point of difference concerns the complexes themselves, and their physical chemical implications. For example, the chemical activity of cholesterol changes markedly at the stoichiometric composition.* The differences are also apparent when our monolayer phase diagrams are compared with those calculated by other research groups (Ipsen et al., 1987; Ipsen and Mouritsen, 1989). Irrespective of the presence or absence of liquid-liquid phase boundaries, the condensed complex picture leads to special properties of the liquid in the region of the stoichiometric composition. Most notably, these properties include abrupt composition-dependent changes in the chemical activity of cholesterol. The calculated chemical activity of cholesterol for one mixture is illustrated in Fig. 8. Note the steep increase in activity in the vicinity of the stoichiometric composition. This effect is unrelated to the coexistence of solid and liquid phases, as shown by the dotted line, for which the solid phase was omitted.

Although the thermodynamic model described here implies little about the molecular structure of the condensed complex, it is worthwhile to note that from a thermodynamic perspective, the complex is akin to a lipid micelle in two dimensions.

In the lipid monolayer studies, the equilibrium constant K_{eq} has an exponential dependence on the monolayer pressure. This dependence is related to the decrease in area (condensation) associated with each molecule of complex formed. That is, in monolayers the equilibrium constant of Eq. 1 can be written as $K_0 \exp(-\pi \Delta A/k_B T)$, where π is the monolayer pressure, K_0 is the equilibrium constant at zero pressure, and ΔA is the change in molecular area for the reaction. Equivalently, the equilibrium constant may be expressed as $\hat{K}_0^n \exp(-n\pi \Delta \hat{A}/k_B T)$, where $\hat{K}_0$ and $\Delta \hat{A}$ are the standard equilibrium constant and area change for the normalized reaction, Eq. 9. The normalized equilibrium constant parameter $\hat{K}_0$ and the cooperativity parameter n are treated as independent parameters. $\Delta \hat{A}$ is also an adjustable parameter, but its magnitude is restricted by experimental data on monolayer areas. In much the same way for bilayers the equilibrium constant is defined by Eqs. 7 and 8, and the parameters $\hat{K}_{eq}^\theta$ and n are treated as independent parameters.

The value of $\Delta \hat{H}_{rxn}$ is set by integration of the experimental broad heat capacity profile, with a small adjustment for the systematic error in the curve-fitting process. As noted earlier, the width of the broad heat absorption restricts the value of n. The value of n that fits the calorimetry best is of the order of magnitude 10, specifically $n \approx 12$, as based on the comparisons of observed widths of the broad heat absorption with calculated values. It should be noted that the larger $\Delta \hat{H}_{rxn}$ values used for the longer phospholipids lead to broadening of the calculated decomposition transition, without any change in n. Values of n of the order of 3–4 have been used in simulating properties of phospholipid monolayers containing cholesterol. It is not surprising that the "best" value for n is higher in bilayers than in monolayers, in view of the likelihood of transbilayer cooperativity. The equilibrium constants used in the present work are of the same order as those appropriate to the monolayer work for applied pressures of say, 20–30 dyne/cm, using area contractions of the order of (30 Å^2)n per complex in the normalized reaction, Eq. 9. Such a pressure corresponds to a molecular density close to that in bilayers (Seelig, 1987). A quantitative comparison of equilibrium constants between the two systems is difficult because the equilibrium constant K_{eq} depends strongly on temperature in bilayers, and on temperature and pressure in monolayers. Quantitative comparisons need to be carried out at the same temperature and molecular density.

A result found in some but not all of our calculations involving condensed complexes has been the requirement of a relatively large cooperativity parameter, n. This has led us to consider the general question of the degree of order in these mixtures. It is possible to generalize the chemical

equilibrium condensed complex model to include complexes with relatively short-range and long-range order. This raises the possibility that the endotherm found in scanning calorimetry may correspond to the melting of complexes having long-range order ($n \gg 10$) to form complexes with the same stoichiometry but with short-range order ($n \approx 10$). The thermal dissociation of the complexes would then be at higher temperatures for each mixture. Calculations of this generalized model will be described elsewhere.

REFERENCES

Anderson, T. G., and H. M. McConnell. 2000. Multiple cholesterol-phospholipid complexes in membranes. *Colloids & Surfaces.* 171:13–23.

Corrales, L. R., and J. C. Wheeler. 1989a. Tetracritical and novel tricritical points in sulfur solutions: a Flory model for polymerization of rings and chains in a solvent. *J. Chem. Phys.* 90:5030–5055.

Corrales, L. R., and J. C. Wheeler. 1989b. Chemical reaction driven phase transitions and critical points. *J. Chem. Phys.* 91:7097–7112.

Dietrich, C., L. A. Bagatolli, Z. N. Volovyk, N. L. Thompson, M. Levi, K. Jacobson, and E. Gratton. 2001. Lipid rafts reconstituted in model membranes. *Biophys. J.* 80:1417–1428.

Engelman, D. M., and J. E. Rothman. 1972. The planar organization of lecithin-cholesterol bilayers. *J. Biol. Chem.* 247:3694–3697.

Feingold, L. 1993. Cholesterol in Membrane Models. CRC Press, Ann Arbor, MI.

Finean, J. B. 1953. Phospholipid-cholesterol complex in the structure of myelin. *Experientia.* 9:17–19.

Finean, J. B. 1990. Interaction between cholesterol and phospholipid in hydrated bilayers. *Chem. Phys. Lipids.* 54:147–156.

Hinz, H., and J. M. Sturtevant. 1972. Calorimetric investigation of the influence of cholesterol on the transition properties of bilayers formed from synthetic L-α-lecithins in aqueous suspension. *J. Biol. Chem.* 247:3697–3700.

Ipsen, J. H., G. Karlstrom, O. G. Mouritsen, H. Wennerström, and M. J. Zuckermann. 1987. Phase equilibria in the phosphatidylcholine-cholesterol system. *Biochim. Biophys. Acta.* 905:162–172.

Ipsen, J. H. and O. G. Mouritsen. 1989. Decoupling of the crystalline and conformational degrees of freedom in lipid monolayers. *J. Chem. Phys.* 91:1855–1865.

Ipsen, J. H., O. G. Mouritsen, and M. J. Zuckermann. 1989. Theory of thermal anomalies in the specific heat of lipid bilayers containing cholesterol. *Biophys. J.* 56:661–667.

Leathes, J. B. 1925. Condensing effect of cholesterol on monolayers. *Lancet.* 208:853–856.

Mabrey, S., P. L. Mateo, and J. M. Sturtevant. 1978. High-sensitivity scanning calorimetric study of mixtures of cholesterol with dimyristoyl- and dipalmitoylphosphatidylcholines. *Biochemistry.* 17:2464–2468.

Marsh, D. 1990. CRC Handbook of Lipid Bilayers. CRC Press, Boca Raton, FL.

McConnell, H. M. 1991. Structures and transitions in lipid monolayers at the air-water interface. *Annu. Rev. Phys. Chem.* 42:171–195.

McMullen, T. P. W., R. N. A. H. Lewis, and R. N. McElhaney. 1993. Differential scanning calorimetric study of the effect of cholesterol on the thermotropic phase behavior of a homologous series of linear saturated phosphatidylcholines. *Biochemistry.* 32:516–522.

Nielsen, M., L. Miao, J. H. Ipsen, M. J. Zuckermann, and O. G. Mouritsen. 1999. Off-lattice model for the phase behavior of lipid-cholesterol bilayers. *Phys. Rev. E.* 59:5790–5803.

Nielsen, M., J. Thewalt, L. Miao, J. H. Ipsen, M. Bloom, M. J. Zuckermann, and O. G. Mouritsen. 2000. Sterol evolution and the physics of membranes. *Europhys. Lett.* 52:368–374.

Presti, F. T., R. J. Pace, and S. I. Chan. 1982. Cholesterol-phospholipid interaction in membranes. 2. Stoichiometry and molecular packing of cholesterol-rich domains. *Biochemistry.* 21:3831–3835.

Radhakrishnan, A., and H. M. McConnell. 1999a. Cholesterol-phospholipid complexes in membranes. *J. Am. Chem. Soc.* 121:486–487.

Radhakrishnan, A., and H. M. McConnell. 1999b. Condensed complexes of cholesterol and phospholipids. *Biophys. J.* 77:1507–1517.

Radhakrishnan, A., and H. M. McConnell. 1999c. Electric field effect on cholesterol-phospholipid complexes. *Proc. Natl. Acad. Sci. USA.* 97:1073–1078.

Radhakrishnan, A., and H. M. McConnell. 2000. Chemical activity of cholesterol in membranes. *Biochemistry.* 39:8119–8124.

Rechtenwald, D. J., and H. M. McConnell. 1981. Phase equilibria in binary mixtures of phosphatidylcholines and cholesterol. *Biochemistry.* 20:4505–4510.

Seelig, A. 1987. Local anesthetics and pressure: a comparison of dibucaine binding to lipid monolayers and bilayers. *Biochim. Biophys. Acta.* 899:196–204.

Somerharju, P., J. A. Virtanen, and K. H. Cheng. 1999. Lateral organization of membrane lipids. The superlattice view. *Biochim. Biophys. Acta.* 1440:32–48.

Sugar, I. P., D. Tang, and P. L. Chong. 1994. Monte Carlo simulation of lateral distribution of molecules in a two-component lipid membrane. Effect of long-range repulsive interactions. *J. Phys. Chem.* 98:7201–7210.

Thewalt, J. L., and M. Bloom. 1992. Phosphatidylcholine:cholesterol phase diagrams. *Biophys. J.* 63:1176–1181.

Vaidya, R. A., and R. D. Hester. 1984. Deconvolution of overlapping chromatographic peaks using constrained non-linear optimization. *J. Chromatog.* 287:231–244.

Vist, M. R., and J. H. Davis. 1989. Phase equilibria of cholesterol/dipalmitoylphosphatidylcholine mixtures: D nuclear magnetic resonance and differential scanning calorimetry. *Biochemistry.* 29:451–464.

Wang, M. M., I. P. Sugar, and P. L. Chong. 1998. Role of the sterol superlattice in the partitioning of the antifungal drug nystatin into lipid membranes. *Biochemistry.* 37:11797–11805.